

Temperature Dependence Measurements and Structural Characterization of Trimethyl Ammonium Ionic Liquids with a Highly Polar Solvent

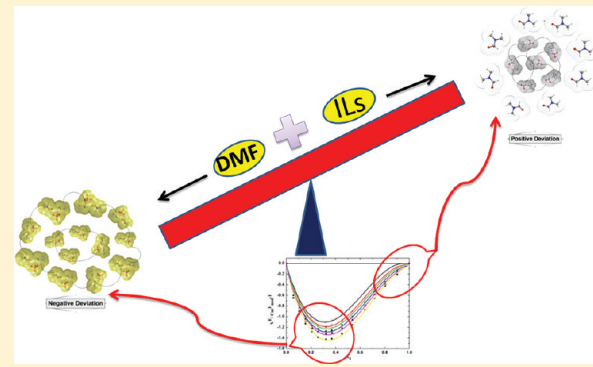
Pankaj Attri,[†] Pannuru Venkatesu,^{*†} and T. Hofman[‡]

[†]Department of Chemistry, University of Delhi, Delhi 110 007, India

[‡]Division of Physical Chemistry, Warsaw, University of Technology, ul. Noakowskiego 3, 00-664 Warszawa, Poland

Supporting Information

ABSTRACT: We report the synthesis and characterization of a series of an ammonium ionic liquids (ILs) containing acetate, dihydrogen phosphate, and hydrogen sulfate anions with a common cation. To characterize the thermophysical properties of these newly synthesized ILs with the highly polar solvent *N,N*-dimethylformamide (DMF), precise measurements such as densities (ρ) and ultrasonic sound velocities (u) over the whole composition range have been performed at atmospheric pressure and over wide temperature ranges (25–50 °C). The excess molar volume (V^E) and the deviation in isentropic compressibilities ($\Delta\kappa_s$) were predicted using these temperature dependence properties as a function of the concentration of ILs. The Redlich–Kister polynomial was used to correlate the results. The ILs investigated in the present study included trimethylammonium acetate $[(\text{CH}_3)_3\text{NH}][\text{CH}_3\text{COO}]$ (TMAA), trimethylammonium dihydrogen phosphate $[(\text{CH}_3)_3\text{NH}][\text{H}_2\text{PO}_4]$ (TMAP), and trimethylammonium hydrogen sulfate $[(\text{CH}_3)_3\text{NH}][\text{HSO}_4]$ (TMAS). The intermolecular interactions and structural effects were analyzed on the basis of the measured and the derived properties. In addition, the hydrogen bonding between ILs and DMF has been demonstrated using semiempirical calculations with help of Hyperchem 7. A qualitative analysis of the results is discussed in terms of the ion–dipole, ion-pair interactions, and hydrogen bonding between ILs and DMF molecules and their structural factors. The influence of the anion of the protic IL, namely, acetate (CH_3COO), dihydrogen phosphate (H_2PO_4), and hydrogen sulfate (HSO_4), on the thermophysical properties is also provided.



INTRODUCTION

The design and synthesis of ionic liquids (ILs) have been one of the ways to accelerate the pace of ILs in large-scale industrial applications and prevent environmental hazards. ILs are performing more promising perspectives in the various fields such as organic synthesis,¹ catalysis or biocatalysis,^{2–4} materials science,⁵ electrochemistry,⁶ separation technology,^{7,8} and preserving the protein stability^{9,10} due to their unique physicochemical properties at the laboratory level and even at the industrial scale.^{11,12} The significant attention that in the past decade the scientific community has shown toward mainly due to the great versatility in cation–anion combinations and favorable unique properties such as high ionic mobility, nonflammability, high potential for recycling, and extremely low vapor pressure.^{13–17} For these reasons, they rapidly gained interest as greener replacements for traditional volatile organic solvents (VOCs). Moreover, ILs have become much popular because of the intensified ion densities, good ionic conductivities, wide electrochemical window, and good thermal stability, and ILs are used as green solvents for biochemistry, polymer chemistry, catalysis reactions, chemical synthesis, and separation science.^{9,10,16–20}

The right choice of the cation–anion pair allows the modulation of physicochemical properties, such as density and ultrasonic sound velocity as well as structural properties of the solvent media, which is markedly controlled both by cation–anion and ion–solvent interaction.²¹ The chemical complexity of the combination of ions of ILs involved in the liquid structure exhibit challenges for theoreticians and chemists to understand the thermophysical properties for mixed solvents of ILs with organic molecular liquids. Studies on thermophysical properties of the pure ILs and their mixtures with polar compounds have shown that the choice of anion or cation has strongly influenced on the molecular characteristics of the different species of ILs.^{15–17,22} To expand basic needs for scientific research and gain some insight into the several aggregations of molecular interactions of ILs with highly polar compounds, we have synthesized different combinations of anions with an ammonium cation of new ILs for our study because this novel kind of ILs appears to be promising for various chemical industrial applications.

Received: June 23, 2011

Revised: July 21, 2011

Published: July 22, 2011

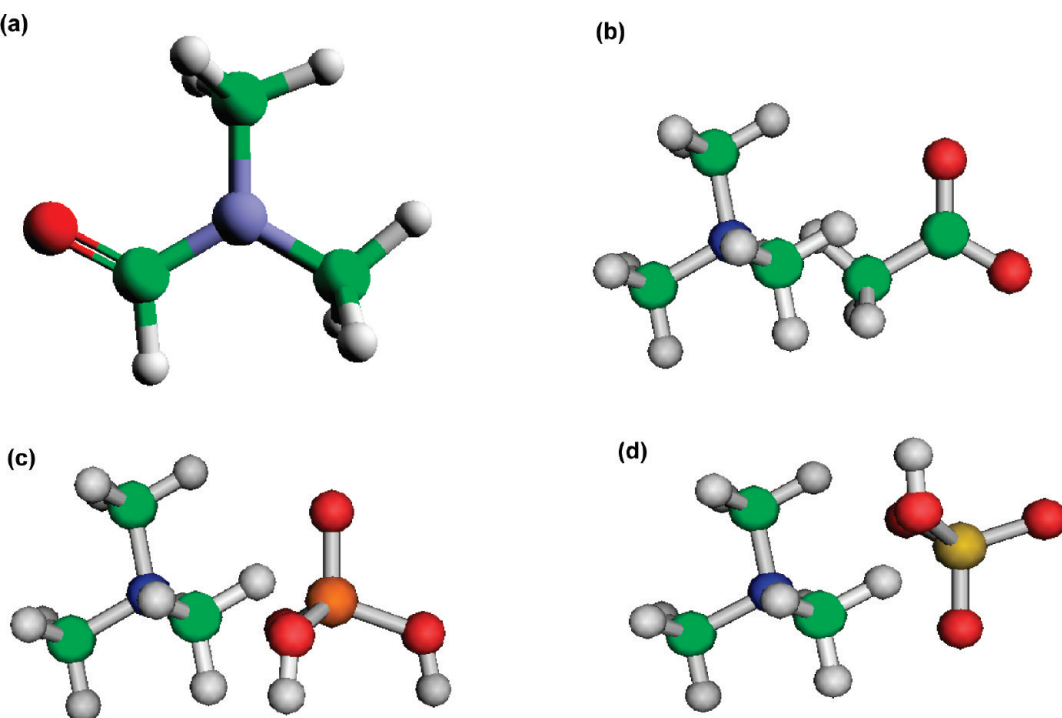
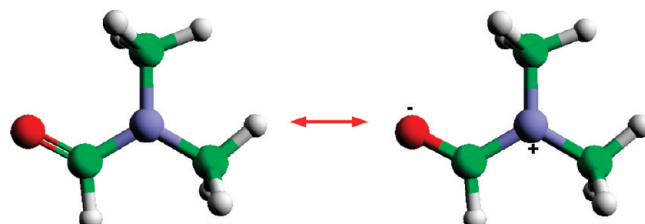


Figure 1. Schematic structures for (a) DMF, (b) TMAA, (c) TMAP, and (d) TMAS. Color representation as green = carbon, white = hydrogen, red = oxygen, and blue = nitrogen.

Thermophysical properties of mixed solvents of ILs with organic molecular liquids are paramount for the design of many technological processes and required for any practical applications.^{23–28} Moreover, experimental data of thermodynamic and thermophysical properties of liquids and liquid mixtures are fascinating and of high fundamental and practical importance for the industry. Although a qualitative connection between the macroscopic and microscopic features is feasible, quantitative conclusions are of interest to both academic and industry communities. In spite of the importance of properties of ILs in different solvent media, only a small amount of physicochemical data is available in the literature, which mainly characterizes ILs.^{29–34} In this context, our aim is to explore closely two key thermophysical properties such as density (ρ) and ultrasonic sound velocity (u) for the mixed solvents of ILs and polar solvent. Up to now, there is no systematic documentation for the trimethyl ammonium ILs with polar solvents.

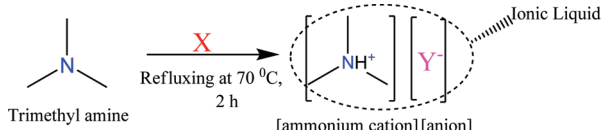
N,N-Dimethylformamide (DMF) is a polar solvent with a high boiling point and is used widely in a variety of industrial processes, including manufacturing of synthetic fibers, leathers, films, and surface coatings.^{35–37} It is also used in the manufacturing of solvent dyes as an important raw material as well as a solvent in peptide coupling for pharmaceuticals, in the development and production of pesticides. DMF is a stable compound with a strong electron pair donating and accepting ability and is widely used in studies on solvent reactivity relationships.^{38–41} DMF is of particular interest because any significant structural effects are absent due to the lack of hydrogen bonds. Therefore, it may be used as an aprotic protophilic solvent with a large dipole moment (μ) of 3.24 D, a high dielectric constant (ϵ) of 36.71 at 25 °C,⁴² and good donor–acceptor properties, which enable it to dissolve a wide range of both organic and inorganic substances. In addition, DMF can serve as a model compound for peptides to

obtain information on protein systems. The resonance structure of DMF is shown below.



In DMF, the presence of two electrons repelling $-\text{CH}_3$ groups make the lone pair at nitrogen still more perceptible toward donation.^{43,44} Thus, it may be argued that the DMF is actually the donor of nitrogen electron pairs. The schematic chemical structures of the DMF as well as ILs are shown in Figure 1.

In view of the wide scope of molecular interactions between DMF with our newly synthesized ammonium ILs, it is essential to study the thermophysical properties to obtain deeper insight into the knowledge of molecular interactions of binary mixtures. Therefore, the present work main pursues the following: (i) to analyze the anion effect over wide ranges of temperature, (ii) to bring in molecular and structural information from an anion/cation features based on the temperature dependence properties of ρ and u as well as derived properties of excess molar volume (V^E) and deviation of isentropic compressibility ($\Delta\kappa_s$), and (iii) to infer the theoretical calculation of the hydrogen bonding between ILs and DMF. We report here the synthesis of trimethyl ammonium ILs, mainly trimethylammonium acetate $[(\text{CH}_3)_3\text{NH}][\text{CH}_3\text{COO}]$ (TMAA), trimethylammonium dihydrogen phosphate $[(\text{CH}_3)_3\text{NH}][\text{H}_2\text{PO}_4]$ (TMAP), and trimethylammonium hydrogen sulfate $[(\text{CH}_3)_3\text{NH}][\text{HSO}_4]$

Scheme 1. Synthesis of Trimethylammonium Ionic Liquids

Where $X = \text{CH}_3\text{COOH}, \text{H}_2\text{SO}_4, \text{H}_3\text{PO}_4$
 $Y = \text{CH}_3\text{COO}^-, \text{HSO}_4^-, \text{H}_2\text{PO}_4^-$

(TMAS). This study intends to draw molecular level information from the macroscopic properties on the molecular interaction between ILs and DMF.

EXPERIMENTAL SECTION

1. Materials. DMF (Aldrich, purity >99.9%) and trimethylamine were purchased from Sigma Chemical Company. The fluids were degassed with ultrasound, kept in the dark over Fluka 0.3 nm molecular sieves for several days, and purified by fractional distillation. The purity of the chemical products was verified by measuring the densities (ρ), refractive indices (n), and sound velocity (u), which were in good agreement with the literature values.⁴² The purities of the samples were further confirmed by the gas–liquid chromatography (GLC) single sharp peaks. All ILs were synthesized^{45,46} in our laboratory, as given below.

2. Preparation of an Ammonium ILs. All ammonium ILs used in this work, namely, TMAA, TMAP, and TMAS, of general type [amine][anion] were synthesized, which is shown schematically in Scheme 1.

3. Synthesis of Trimethylammonium Acetate (TMAA). The synthesis of TMAA was carried out in a 250 mL round-bottomed flask, which was immersed in a water bath and fitted with a reflux condenser. Acetic acid (1 mol) was added dropwise to a trimethylamine (1 mol) at 70 °C for 1 h. The reaction mixture was heated at 80 °C under vigorous stirring for 2 h to ensure that the reaction had proceeded to completion. The reaction mixture was then dried at 80 °C until the weight of the residue remained constant. The sample was analyzed by Karl Fisher titration revealed very low levels of water (below 70 ppm). The yield of TMAA was 98%. ^1H NMR (DMSO- d_6): δ (ppm) 2.51 (s, 1H), 2.10 (s, 3H). HRMS calculated for $\text{C}_5\text{H}_{13}\text{NO}_2$ 119.09, found 119.05.

4. Synthesis of Trimethylammonium Dihydrogen Phosphate (TMAP). The similar procedure as that described above for TMAA was followed with the exception of the use of phosphoric acid [anion] instead of acetic acid. The yield of TMAP was 97%. ^1H NMR (DMSO- d_6): δ (ppm) 2.51 (s, 9H), 2.74 (s, 1H). HRMS calculated for $\text{C}_3\text{H}_{12}\text{NO}_4\text{P}$ 157.05, found 157.02. Melting point: 116 °C.

5. Synthesis of Trimethylammonium Hydrogen Sulfate (TMAS). The similar procedure as that delineated above for TMAA was followed with the exception of the use of sulfuric acid [anion] instead of acetic acid. The yield of TMAS was 98%. ^1H NMR (DMSO- d_6): δ (ppm) 2.52 (s, 9H), 2.75 (s, 1H). HRMS calculated for $\text{C}_3\text{H}_{11}\text{NO}_4\text{S}$ 157.04, found 157.01. Melting point: 129 °C.

The molecular weight, normal purity, density, and ultrasonic sound velocities of ILs and DMF, which are studied in the present work, are summarized in Table 1.

Table 1. Solvent Purity, Molecular Weight (MW), Density (ρ), and Ultrasonic Sound Velocity (u) for the Solvents such as ILs and DMF at Various 25 °C and at Atmospheric Pressure

solvent	MW (g·mol ⁻¹)	purity	ρ (g·cm ⁻³)	u (m·s ⁻¹)
DMF	73.05	99%	0.94385	1456
TMAA	119.05	99%	1.05385	1544
TMAP	157.02	99%	1.35361	1672
TMAS	157.01	99%	1.35361	1672

METHODS

1. Density Measurements. The density measurements of pure compounds and ILs + DMF were performed with an Anton-Paar DMA 4500 M vibrating-tube densimeter, equipped with a built-in solid-state thermostat and a resident program with accuracy of temperature of ± 0.03 °C. Typically, density precisions are 0.00005 g·cm⁻³. The instrument was calibrated once a day with double-distilled, deionized water and with air as standards. The excess molar volumes (V^E) (± 0.003 cm³·mol⁻¹) of ILs with DMF systems over the IL concentration range at different temperatures have been deduced from the densities of the pure compounds and mixture (ρ_m) using the standard equations.

2. Ultrasonic Sound Velocity Measurements. Ultrasonic sound velocities were measured by a single crystal ultrasonic interferometer (model F-05) from Mittal Enterprises, New Delhi, India, at a 2 MHz frequency at various temperatures. Prior to measurements, the interferometer was calibrated at 25 °C with double-distilled water and purified methanol. A thermostatically controlled, well-stirred circulated water bath with a temperature controlled to ± 0.01 °C was used for all of the ultrasonic sound velocity measurements for pure components and mixtures. The uncertainty of sound velocity is 0.02%.

3. NMR Measurements. The purity of ILs was proved by ^1H NMR analysis. ^1H (400 MHz) spectra were recorded on a JEOL 400 NMR spectrometer in DMSO- d_6 .

Clear solutions were prepared gravimetrically using a Mettler Toledo balance with a precision of ± 0.0001 g. The uncertainty in solution composition expressed in mole fraction was found to be less than $5 \cdot 10^{-4}$. The mixing of the two components was promoted by the movement of a small glass sphere (inserted in the vial prior to the addition of the ILs) as the flask was slowly and repeatedly inverted. After mixing the sample, the bubble-free homogeneous sample was transferred into the U-tube of the densimeter or the sample cell of ultrasonic interferometer through a medical syringe.

4. Hydrogen Bonding through Simulation Program. The structures of ILs and of DMF were optimized based on molecular mechanics and semiempirical calculations using the HyperChem 7 Molecular Visualization and Simulation program.⁴⁷ Geometry optimizations based on molecular mechanics (using the MM+ force field) and semiempirical calculations were used to find the coordinates of molecular structures that represent a potential energy minimum. For geometry optimization using both molecular mechanics and semiempirical calculations, the Polak–Ribiere routine with a root-mean-square (rms) gradient of 0.01 as the termination condition was used. The minimum distance between solvent molecules and solute atoms was set at 2.3 Å. Molecular dynamics calculations were used to obtain a lower

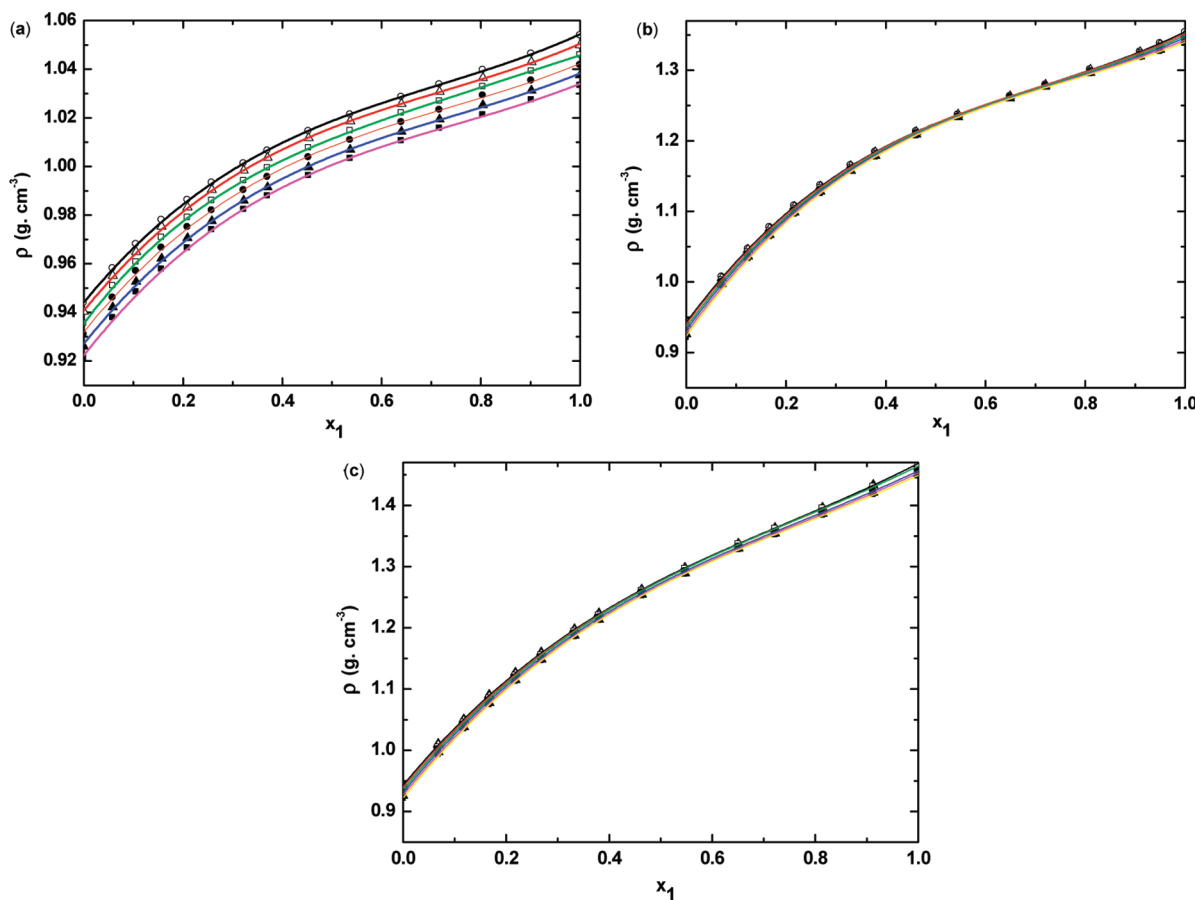


Figure 2. Temperature dependence of densities for the mixtures of ILs with DMF vs mole fraction of IL x_1 for (a) TMAA $\{(x_1) 25\text{ }^\circ\text{C} (\circ), (x_1) 30\text{ }^\circ\text{C} (\triangle), (x_1) 35\text{ }^\circ\text{C} (\square), (x_1) 40\text{ }^\circ\text{C} (\bullet), (x_1) 45\text{ }^\circ\text{C} (\blacktriangle), \text{ or } (x_1) 50\text{ }^\circ\text{C} (\blacksquare)\} + \text{DMF } (x_2)$, (b) TMAP $\{(x_1) 25\text{ }^\circ\text{C} (\circ), (x_1) 30\text{ }^\circ\text{C} (\triangle), (x_1) 35\text{ }^\circ\text{C} (\square), (x_1) 40\text{ }^\circ\text{C} (\bullet), (x_1) 45\text{ }^\circ\text{C} (\blacktriangle), \text{ or } (x_1) 50\text{ }^\circ\text{C} (\blacksquare)\} + \text{DMF } (x_2)$, (c) TMAS $\{(x_1) 25\text{ }^\circ\text{C} (\circ), (x_1) 30\text{ }^\circ\text{C} (\triangle), \text{ or } (x_1) 35\text{ }^\circ\text{C} (\square), (x_1) 40\text{ }^\circ\text{C} (\bullet), (x_1) 45\text{ }^\circ\text{C} (\blacktriangle), \text{ or } (x_1) 50\text{ }^\circ\text{C} (\blacksquare)\} + \text{DMF } (x_2)$ at various compositions and at atmospheric pressure. The solid line represents the smoothness of these data.

energy minimum by enabling molecules to cross potential barriers.^{48,49} For the structures of ILs optimized using semiempirical calculations, single point calculations were carried out to determine the total energies and heats of formation.

RESULTS AND DISCUSSION

Our experimental ρ and u values for a series of trimethyl ammonium ILs with DMF were obtained at atmospheric pressure for the whole concentration range at temperatures from 25 to 50 °C in steps of 5 °C. The values of ρ and u are presented in Table 1 (Supporting Information), for ILs, DMF, and their mixtures as a function of IL concentration. Virtually, ILs are miscible with medium- to high-dielectric liquids and immiscible with low dielectric liquids.⁵⁰ In the present study, all ILs are completely miscible in DMF ($\epsilon = 36.71$ at 25 °C),⁴² since DMF is a high dielectric liquid. It is seen that the ρ or u (up to ≈ 0.4000 mole fraction of IL, later the u values decrease) of the mixtures increase with increasing concentrations of the IL in DMF, as shown in Figures 2 or 3, respectively. The effect of the ILs on the ρ and u in the DMF has been examined at various temperatures. As it can be observed, the ρ and u sharply decreases as the temperature increases in the three systems. There are no previous ρ and u data reported in the literature for ammonium ILs + DMF at various temperatures for comparison. It is obvious

that the both ρ and u values reflect the structural properties of liquids and packing factors of the system. A careful examination of Figure 2 reveals that the acetate IL system shows lower densities than HSO₄ or H₂PO₄ anion IL systems. The HSO₄ and H₂PO₄ anion systems display the highest density values due to increased the size of the anion. For the sake of clarity and comparison between three ILs, the ρ and u values of IL + DMF over the whole composition range at 25 °C have presented in Figure 4.

Usually, the densities of the ILs containing the same cation increase with increasing molecular weight of the associated anion.⁵¹ Fredlake and co-workers⁵² observed that this behavior is quite consistent for anions and pointed out that anions are small enough to easily occupy a position closer to the relatively large cation. The difference in density between IL (different anions) systems can be explained by the different sizes of the associated with same cation. In this context, the results in Figure 4 clearly show that the density values of the TMAS + DMF mixtures are higher, when compared to the mixtures of the TMAP + DMF and TMAA + DMF. However, the TMAS + DMF and TMAP + DMF mixtures have almost same density from the mole fraction of IL 0 to ≈ 0.2000 . The lower densities of TMAA + DMF than other two systems are due to weaker intermolecular interactions of the relatively larger TMAS or TMAP with DMF. The large size of the (dihydrogen phosphate \approx hydrogen sulfate $>$ acetate)

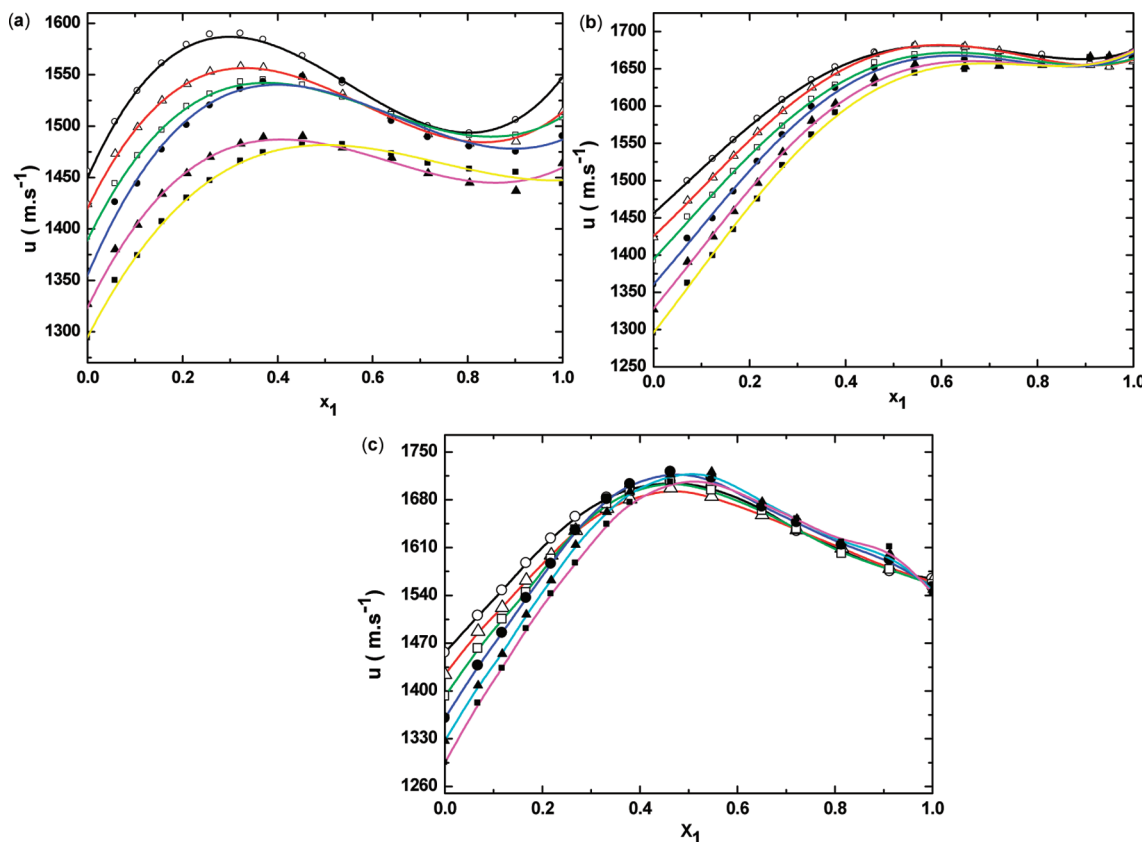


Figure 3. Temperature dependence of ultrasonic sound velocity for the mixtures of ILs with DMF vs mole fraction of IL x_1 for (a) TMAA $\{(x_1) 25^\circ\text{C} (\circ), (x_1) 30^\circ\text{C} (\triangle), (x_1) 35^\circ\text{C} (\square), (x_1) 40^\circ\text{C} (\bullet), (x_1) 45^\circ\text{C} (\blacktriangle), \text{ or } (x_1) 50^\circ\text{C} (\blacksquare) + \text{DMF } (x_2)\}$, (b) TMAP $\{(x_1) 25^\circ\text{C} (\circ), (x_1) 30^\circ\text{C} (\triangle), (x_1) 35^\circ\text{C} (\square), (x_1) 40^\circ\text{C} (\bullet), (x_1) 45^\circ\text{C} (\blacktriangle), \text{ or } (x_1) 50^\circ\text{C} (\blacksquare) + \text{DMF } (x_2)\}$, (c) TMAS $\{(x_1) 25^\circ\text{C} (\circ), (x_1) 30^\circ\text{C} (\triangle), (x_1) 35^\circ\text{C} (\square), (x_1) 40^\circ\text{C} (\bullet), (x_1) 45^\circ\text{C} (\blacktriangle), \text{ or } (x_1) 50^\circ\text{C} (\blacksquare) + \text{DMF } (x_2)\}$ at various compositions and at atmospheric pressure. The solid line represents the smoothness of these data.

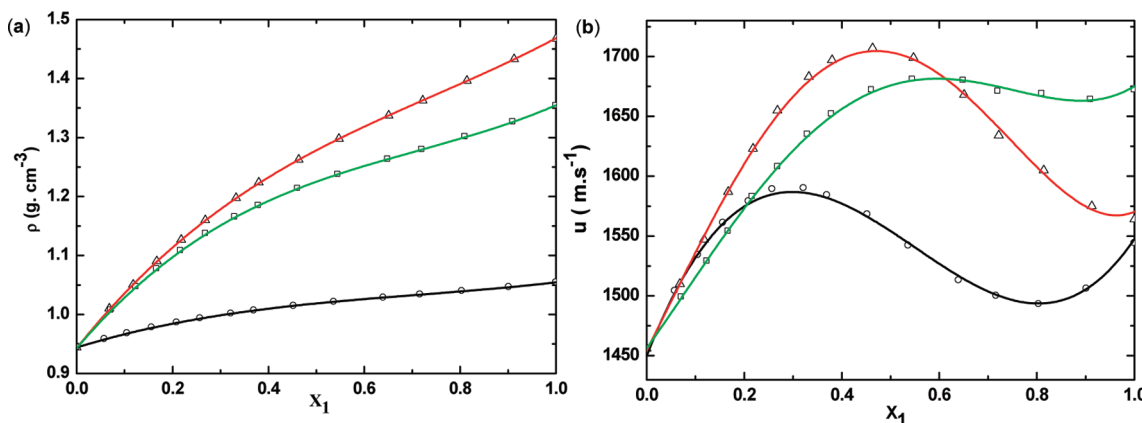


Figure 4. (a) Densities and (b) ultrasonic sound velocity for the mixtures of ILs with DMF vs mole fraction of IL (x_1) for TMAA (\circ), TMAP (\square), and TMAS (\triangle) with DMF (x_2) at 25 °C.

anion shows higher density values than lower sizes of the anion. However, in the case of the TMAA mixture there is no sharp increase in ρ as compared to other two ILs mixtures. In other words, we can state that the density does not increase sharply at a mole fraction of IL (0.3000 to 0.6000), which might be due to a decrease in the ion-pair interaction between these TMAA and DMF. We observed the ρ values to be higher in the

TMAS mixture, lower in the TMAA, and moderate in the TMAP mixture. These discrepancies are varying from IL to IL and solvent to solvent and also depending on the nature as well as the structural arrangement of IL and solvent. The density generally decreases with the increasing size of a cation or anion as documented earlier for ILs.^{53,54} However, this conclusion is not consistent with observations of the present study. As

Table 2. Estimated Parameters of eq 1 and Standard Deviation, σ for the Systems of ILs with DMF at Various Temperatures

Y	system	T/°C	a_0	a_1	a_2	a_3	a_4	σ
$V^E/(cm^3 \cdot mol^{-1})$	TMAA + DMF	25	-3.4416	4.3758	-0.5796			0.008
		30	-3.8409	4.335	-0.7886			0.019
		35	-4.0758	3.9618	0.1536	0.9883	-2.2253	0.011
		40	-4.3148	3.864	0.0303	1.2230	-2.7491	0.012
		45	-4.5481	3.7770	-0.0681	1.5143	-2.9160	0.010
	TMAS + DMF	50	-4.9934	4.0008	0.4574	1.2613	-3.9223	0.015
		25	-8.8735	12.6845	-1.2599			0.040
		30	-9.5491	12.5285	-2.1527			0.059
		35	-10.2493	12.5706	-2.5901			0.067
		40	-11.1079	12.7476	-2.7307			0.081
$\Delta\kappa_s/(T \cdot Pa^{-1})$	TMAP + DMF	45	-11.6467	12.8164	-3.6176			0.088
		50	-12.9151	12.3590	0.9669	2.6815	-8.6559	0.058
		25	-11.2067	15.8373				0.028
		30	-12.1057	15.3037	-1.6982			0.034
		35	-12.8528	15.3194	-2.6305			0.057
	TPAH + DMF	40	-13.6303	15.3711	-3.3493			0.075
		45	-15.2173	13.9281	1.9091	3.6264	-9.7122	0.055
		50	-16.1652	15.5084	0.8131	-8.6173	-10.0261	0.055
		25	-168.78	439.93	-40.59			0.55
		30	-231.95	355.28	18.77	44.21	-127.27	0.65
$\rho/(g \cdot cm^{-3})$	TMAA + DMF	35	-261.52	364.03	-76.13			1.62
		40	-299.01	354.22	28.12	59.89	-193.29	1.08
		45	-341.92	358.16	-99.13			2.44
		50	-375.21	365.19	-109.83			3.04
		25	-366.91	261.81	-22.91			0.59
	TMAS + DMF	30	-423.23	282.17	-25.06			0.93
		35	-464.37	294.65	40.94	63.12	-193.65	1.19
		40	-508.42	351.85	-66.85			2.62
		45	-567.37	380.22	83.63	-20.82	-356.85	1.72
		50	-630.76	409.19	66.76	-41.41	-404.95	1.92
	TMAP + DMF	25	-482.15	336.98				0.816
		30	-515.46	351.62	-67.12			1.46
		35	-589.78	407.95	-74.17			2.01
		40	-661.82	459.14	-112.47			2.21
		45	-742.34	494.69	722.67	-67.80	-408.08	1.66
		50	-801.05	520.87	74.93	-46.46	-566.66	1.36

expected, TMAS or TMAP + DMF mixtures show a very slight difference in their densities, since both of the ILs have the almost same molar mass. These results execute that the anion of ILs plays a key role in the density of mixtures.

Temperature-dependent u values of ILs with DMF were measured starting at 25 °C and increasing the temperature in steps of 5 °C up to 50 °C, and these u data displayed in Figure 3 as a function of IL concentration under atmospheric pressure. The values of u were found to decrease with an increase in temperature, while u values increase with an increase in mole fraction of IL up to ≈0.4500 except in the mixture of TMAA with DMF, whereas in the case of TMAA the u values sharply increase up to ≈0.3200 mole fraction of TMAA. In the case of TMAP or TMAS + DMF, u values increase up to ≈0.4200 of IL, and later the u values decrease up to 0.9900 mole fraction of IL at all investigated temperatures. The anionic sound velocity effect is most obvious, since we have a common cation, resulting in significantly higher u values for the larger anion size of IL systems,

when compared to the smaller size of acetate anion IL systems (Figure 3) at all studied temperatures. Therefore, our result demonstrates that the influence of the anion is significantly affected on ammonium IL–solvent interactions. As seen from Figure 4b, the sound velocity of TMAP with DMF at 25 °C rapidly increases with the increasing composition of IL up to ≈0.4000 mole fraction, and later the u values slightly increased. On the other hand, in the case of TMAS with DMF there is a rapid increase in u values up to the mole fraction ≈0.4300 of TMAS; later the values suddenly decreased up to 0.9900 mole fraction of IL at 25 °C. The progressive weakening of the ion–ion bonds is probably the reason for decrease in u ≈ 0.4000 mole fraction of IL, in all cases except the TMAA system.

Fascinating results are seen in the case of TMAA for which its u values rapidly enhance a ≈0.2000 mole fraction of IL; further a decrease is noted up to 0.8000 mole fraction of IL, and later the values sharply increasing up to mole fraction 0.9800 of TMAA. This may be due to the self-interaction occurring between the

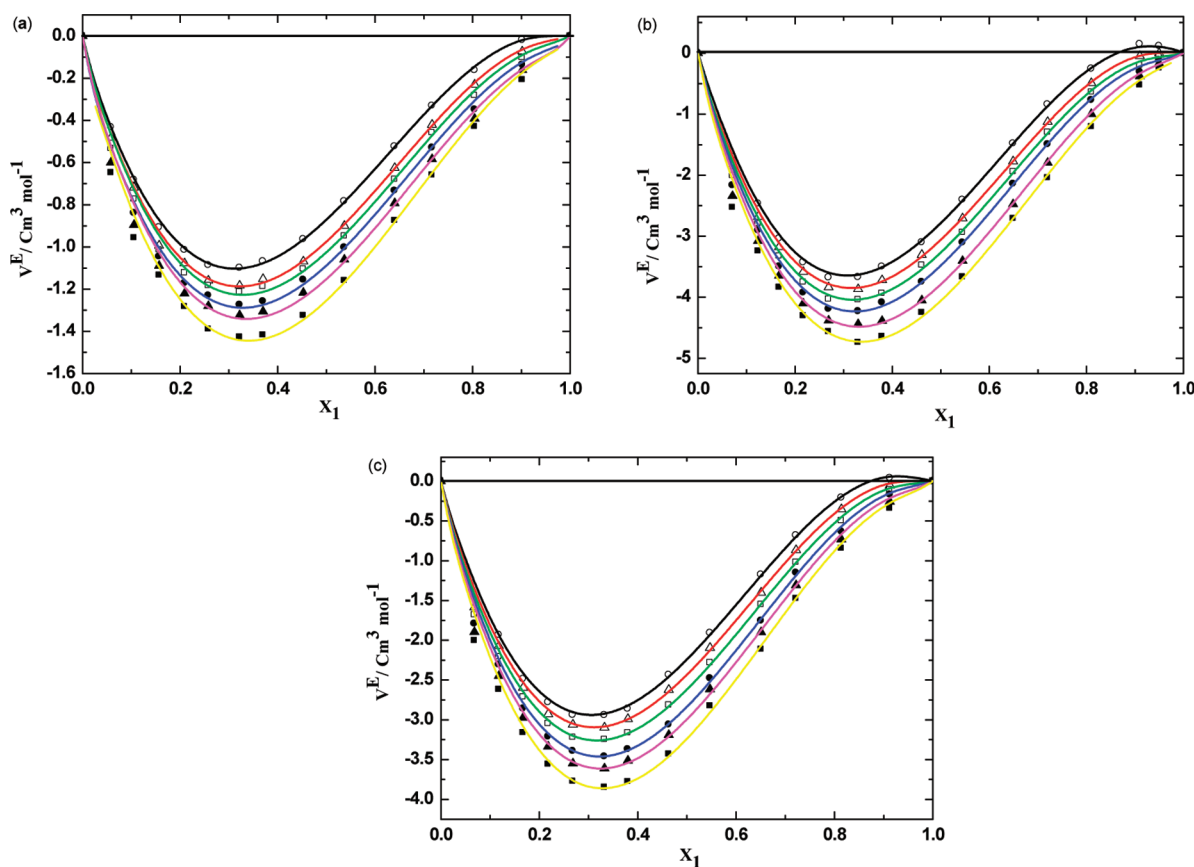


Figure 5. Concentration dependence of excess molar volumes (V^E) against the mole fraction of ILs (a) TMAA $\{(x_1) 25\text{ }^\circ\text{C} (\circ), (x_1) 30\text{ }^\circ\text{C} (\triangle), (x_1) 35\text{ }^\circ\text{C} (\square), (x_1) 40\text{ }^\circ\text{C} (\bullet), (x_1) 45\text{ }^\circ\text{C} (\blacktriangle), \text{ or } (x_1) 50\text{ }^\circ\text{C} (\blacksquare)\} + \text{DMF } (x_2)\}, (b) TMAP $\{(x_1) 25\text{ }^\circ\text{C} (\circ), (x_1) 30\text{ }^\circ\text{C} (\triangle), (x_1) 35\text{ }^\circ\text{C} (\square), (x_1) 40\text{ }^\circ\text{C} (\bullet), (x_1) 45\text{ }^\circ\text{C} (\blacktriangle), \text{ or } (x_1) 50\text{ }^\circ\text{C} (\blacksquare)\} + \text{DMF } (x_2)\}, (c) TMAS $\{(x_1) 25\text{ }^\circ\text{C} (\circ), (x_1) 30\text{ }^\circ\text{C} (\triangle), (x_1) 35\text{ }^\circ\text{C} (\square), (x_1) 40\text{ }^\circ\text{C} (\bullet), (x_1) 45\text{ }^\circ\text{C} (\blacktriangle), \text{ or } (x_1) 50\text{ }^\circ\text{C} (\blacksquare)\} + \text{DMF } (x_2)\}$ at atmospheric pressure. Solid (—) lines are correlated by the Redlich–Kister equation.$$

TMAA molecules. Figure 4 illustrated that the TMAP IL exhibits higher u values up to ≈ 0.4000 mole fraction followed by TMAS than TMAP and least in TMAA with DMF at $25\text{ }^\circ\text{C}$. This is a somewhat surprising result, since one would expect at first view that, as the anion varies from acetate ion to sulfate ion, the overall contribution increases up to ≈ 0.5000 . This shows that there is a significant effect of ρ on the u ; as the density increases, the sound velocity also increases.

Excess molar volumes (V^E) as well as ultrasonic studies are known to provide useful insights into solution structural effects and intermolecular interactions between component molecules. The extent of deviation of liquid mixtures from ideal behavior is best expressed by excess functions. Among them, the excess volumes can be interpreted in three areas, namely, physical, chemical, and structural effects.^{16,17,35} Volumetric properties of binary mixtures of ILs with polar compounds are contribute to the clarification of the various intermolecular interactions existing between the different species found in solution. The excess volumes are determined from the density of pure compounds (ρ_1 and ρ_2) and mixture (ρ_m) using a standard equation.³⁹

The ultrasonic studies have been adequately employed in understanding the nature of molecular interaction in solvent mixed systems. In the chemical industry, a knowledge of the ultrasonic and its related properties of solutions is essential in the design involving chemical separation, heat transfer, mass transfer, and fluid flow. Isentropic compressibilities (κ_s) of the binary

mixtures were calculated using the relation from ρ and u . The detailed procedure of obtaining of κ_s and deviation in isentropic compressibility ($\Delta\kappa_s$) was delineated in our previous papers.^{16,17,39} The composition dependence of the V^E and $\Delta\kappa_s$ properties represents the deviation from ideal behavior of the mixtures and provides an indication of the interactions between IL and DMF. The following Redlich–Kister expression was used to correlate these properties:

$$Y = x_1 x_2 \left(\sum_{i=0}^n a_i (x_1 - x_2)^i \right) \quad (1)$$

where Y refers to V^E or $\Delta\kappa_s$, a_i are adjustable parameters and can be obtained by least-squares analysis. Values of the fitted parameters are listed in Table 2 along with the standard deviations of the fit. The values of V^E and $\Delta\kappa_s$ for the binary mixtures at various temperatures as a function of IL concentration are included in Table 1. Figures 5 and 6 display the experimental data for the binary mixtures, and the fitted curves, along with the excess properties of V^E and $\Delta\kappa_s$, respectively, for the DMF with ILs as a function of IL concentration at different temperatures.

As can be seen in Figure 5, the V^E values have a broad minimum at the composition around ≈ 0.3000 mole fraction of all ILs, for all three binary mixtures at all investigated temperatures. However, we observed that the V^E values present a maximum at $x_1 \approx 0.91$ for the systems of TMAP or TEAS with DMF at $25\text{ }^\circ\text{C}$ only. The minimum increases, and the maximum

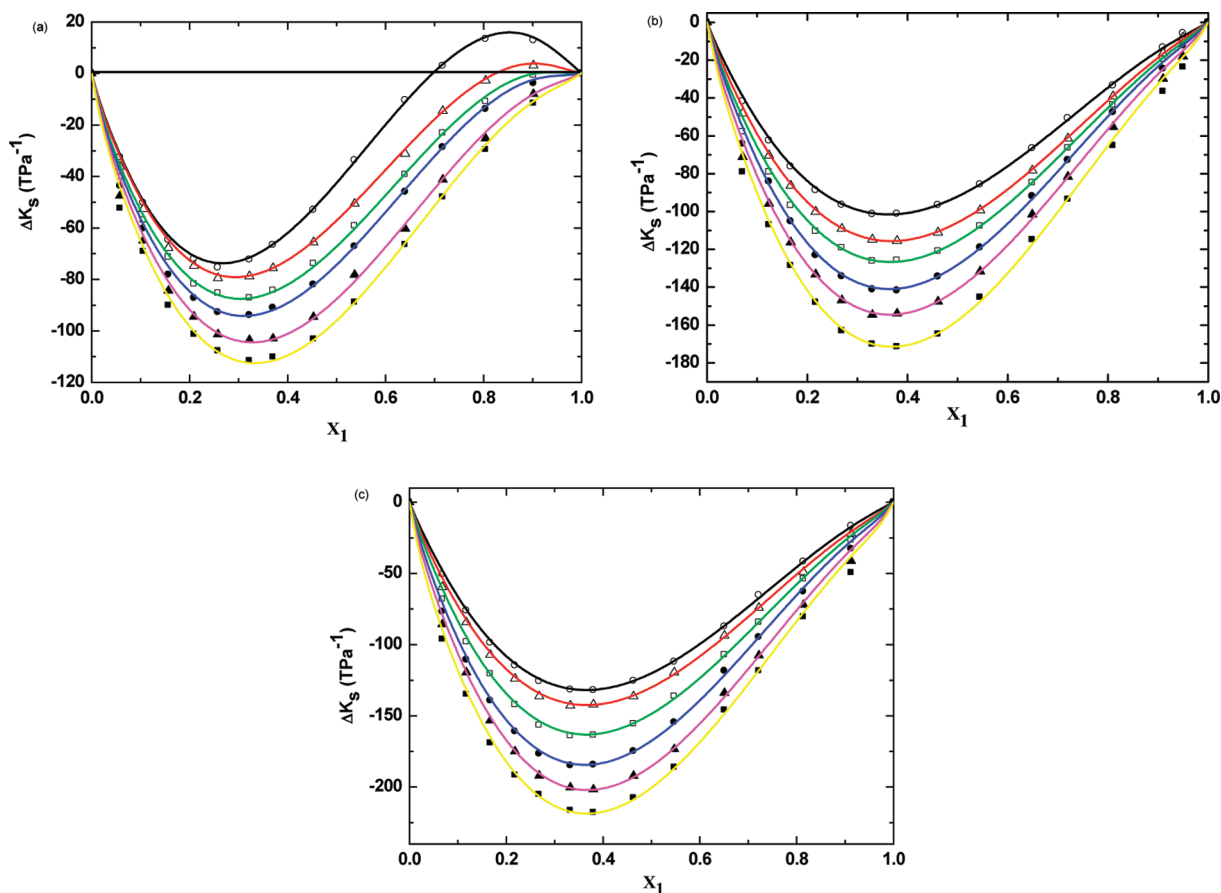


Figure 6. Concentration dependence of deviation in isentropic compressibilities ($\Delta\kappa_s$) against the mole fraction of ILs (a) TMAA $\{(x_1) 25^\circ\text{C} (\circ), (x_1) 30^\circ\text{C} (\triangle), (x_1) 35^\circ\text{C} (\square), (x_1) 40^\circ\text{C} (\bullet), (x_1) 45^\circ\text{C} (\blacktriangle), \text{ or } (x_1) 50^\circ\text{C} (\blacksquare)\} + \text{DMF } (x_2)\}$, (b) TMAP $\{(x_1) 25^\circ\text{C} (\circ), (x_1) 30^\circ\text{C} (\triangle), (x_1) 35^\circ\text{C} (\square), (x_1) 40^\circ\text{C} (\bullet), (x_1) 45^\circ\text{C} (\blacktriangle), \text{ or } (x_1) 50^\circ\text{C} (\blacksquare)\} + \text{DMF } (x_2)\}$, (c) TMAS $\{(x_1) 25^\circ\text{C} (\circ), (x_1) 30^\circ\text{C} (\triangle), (x_1) 35^\circ\text{C} (\square), (x_1) 40^\circ\text{C} (\bullet), (x_1) 45^\circ\text{C} (\blacktriangle), \text{ or } (x_1) 50^\circ\text{C} (\blacksquare)\} + \text{DMF } (x_2)\}$ at atmospheric pressure. Solid (—) lines are correlated by the Redlich-Kister equation.

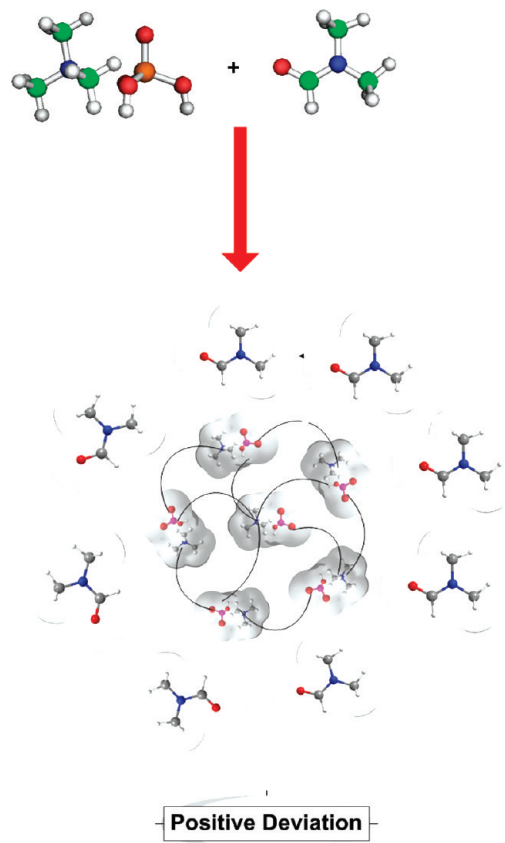
decreases (except TMAA systems) as temperature increases for all three systems. This behavior can be explained because hydrogen bonding is certainly more T -dependent than Coulombic interactions. The minimum can be due to hydrogen bonds between DMF molecules and IL. At higher concentrations of IL, the dissociation of the ions forming the ILs and loss of dipolar interactions of DMF. Moreover, the V^E values are positive for IL-rich compositions and negative for DMF-rich compositions for the mixture of TMAP or TMAS with DMF at 25 °C. The decrease in the magnitude of the negative V^E values with an increase in IL composition can be attributed to the decrease of hydrogen bonding. Although it can also be understood as an increase in the concentration of the IL, a decrease of packing efficiency between IL and DMF contributes to positive deviation for TMAP or TMAS with DMF at 25 °C. For this behavior our assumption is that at a higher concentration of IL some extensive self-association through hydrogen bonding or ion–ion interaction might be occurring. This information is represented as schematically in Scheme 2.

The experimental results in Figure 5 show that the values of V^E for DMF with TMAA are negative over the whole concentration range at all investigated temperatures. Figure 5 parts b and c, depict that, at lower temperatures (25 °C), the V^E values for the system TMAP or TMAS with DMF exhibits an inversion in the sign from negative to positive deviation, indicating that the

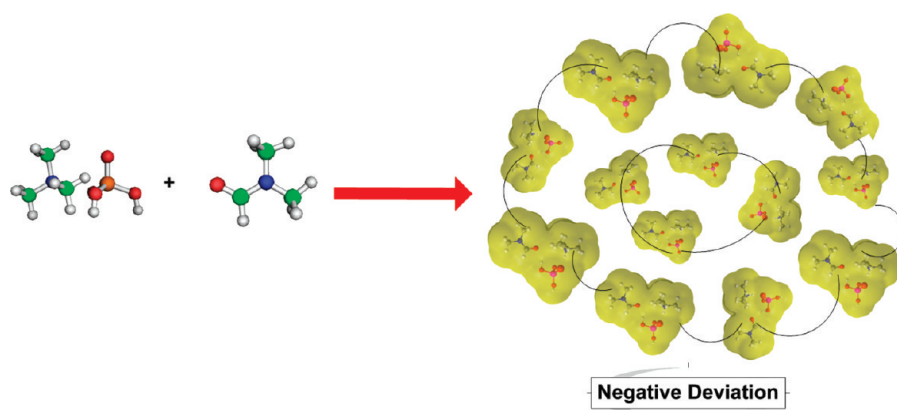
interaction between TMAP or TMAS and DMF decreases as the concentration of IL increases at this temperature. It can be seen that the V^E values are negative in the entire range of composition at 30–50 °C for TMAP or TMAS with DMF. This might be due to the fact that the large difference between molar volumes of the DMF and TMAP or TMAS implies that it is possible that the relatively small organic molecules fit into the interstices upon mixing at all studied temperatures except 25 °C. Therefore, the filling effect of organic molecular liquids in the interstices of ILs and the ion–dipole interactions between organic molecular liquid and ILs all contribute to the negative values of V^E . The negative V^E values reveal that a more efficient packing or attractive interaction occurred when these IL and DMF were mixed at all cases. DMF (oxygen ion of resonating structure of DMF) forms a hydrogen bond with cation, while the other part of the DMF resonating structure (non-hydrogen bonding) interacts more strongly with the anion of the IL. These interactions are shown schematically in Scheme 3. The interactions between the DMF molecules and the ions of IL are due to ion–dipole interactions. This will reduce the hydrogen bonding between the cation and the anion in the IL, which contributes to the negative V^E values. A careful examination of Figure 5 explains that V^E values are significantly at each investigated temperature over the whole mole fraction range of all ammonium ILs with DMF systems. The observed V^E values for all three systems

appear to increase sharply with increasing temperature, which shows the deviation from ideal behavior to become pronounced as the temperature is enhanced. These observations can be depicted to the inherent complexity of the IL with DMF systems as far as interactions with in the system are concerned. On the other hand, the hydrogen bonding between the IL + DMF (Scheme 3) would result in volume contraction, and thereby the V^E values contribute to the negative sign. Obviously, the

Scheme 2. Schematic Depiction of Interactions between ILs + DMF at Various Temperatures for the Positive Deviation Where Color Representation Is the Following, Green = Carbon, White = Hydrogen, Red = Oxygen, and Blue = Nitrogen



Scheme 3. Schematic Depiction of Interactions between ILs + DMF at Various Temperatures for the Negative Deviation Where Color Representation Is the Following, Green = Carbon, White = Hydrogen, Red = Oxygen, and Blue = Nitrogen



contraction in volume of the mixture may be contributed to the weakening the hydrogen-bond interactions between IL molecules with DMF particles and, as a result, a slight increase in the absolute values of V^E values with increasing the temperature of the mixture.

Clearly, the observed negative V^E values decrease further with increasing the temperature in the entire mole fraction range for all three IL systems. It is interesting note that the V^E values in the TMAP + DMF mixture shows more negative values of V^E than the TMAS + DMF and TMAA + DMF mixtures at 25 °C over the entire concentration range (Figure 7a), implying that in the TMAP there are ion–dipole interactions and packing effects with DMF that are stronger than those in the TMAS and TMAA solution at $x_1 \approx 0.2500$. Furthermore, the observed positive values at IL-rich compositions show that there exists no specific interactions between unlike molecules, and also the compact structure of the polar component (DMF) due to dipolar association has been broken by these ILs at rich-IL region (Figure 7a). The magnitude and sign of V^E values are a reflection of the type of interactions taking place in the mixture, which are the result of different effects containing the loss of the DMF dipole interaction from each other (positive V^E) and the breakdown of the IL ion-pair (positive V^E). The interaction between the ion-pair of ILs increases as compared to IL + DMF interactions, which leads to a positive contribution at higher IL concentrations. Interestingly, the hydrogen bonding between ILs and DMF has predicted using semiempirical calculations with the help of Hyperchem 7, and those interactions are explicitly elucidated in Figures 8–10. Our interpretation of hydrogen bonding between of IL and DMF molecules (based V^E data) is quite corroborated with our theoretical calculation of hydrogen bonding of IL + DMF molecules. It is noteworthy to compare the negative deviation of V^E values of TMAA + DMF with TEAS + DMF and TMAP + DMF, which suggests that there is a difference of the anion in all ILs, leading to variation in the hydrogen bond between the ion and DMF molecules (Figures 8–10).

In Figure 6, the $\Delta\kappa_s$ values for ILs + DMF at a wide range of temperatures and atmospheric pressure are illustrated over whole composition range, as a function of IL mole fraction. It can be seen from Figure 6 that the $\Delta\kappa_s$ values for all the systems are negative over the entire composition range and at all investigated temperatures, except in TMAA + DMF systems. However, the observed $\Delta\kappa_s$ values exhibit positive values for the mixture of

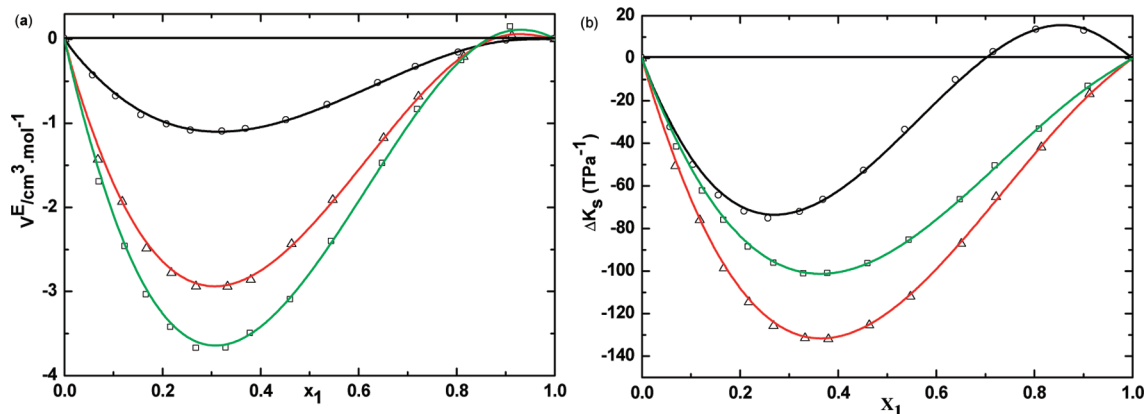


Figure 7. (a) Excess molar volumes (V^E) against the mole fraction of ILs for TMAA (\circ), TMAP (\square), and TMAS (\triangle) at 25 °C and (b) deviation in isentropic compressibilities ($\Delta\kappa_s$) against the mole fraction of ILs for TMAA (\circ), TMAP (\square), and TMAS (\triangle) at 25 °C.

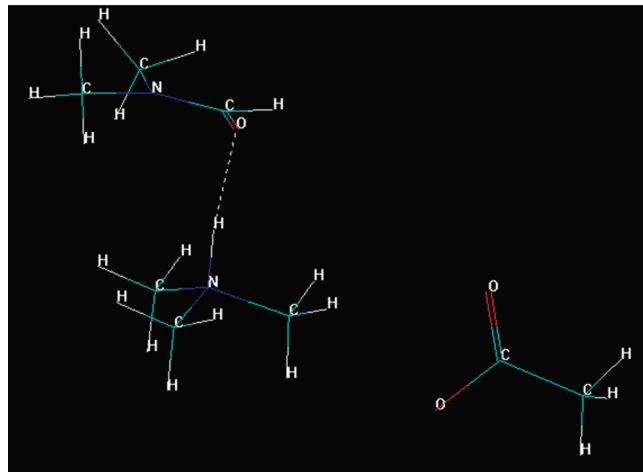


Figure 8. Schematic depiction of the hydrogen bonding interaction between TMAA and DMF molecules, which is predicted by a semi-empirical calculation with the help of Hyperchem 7.

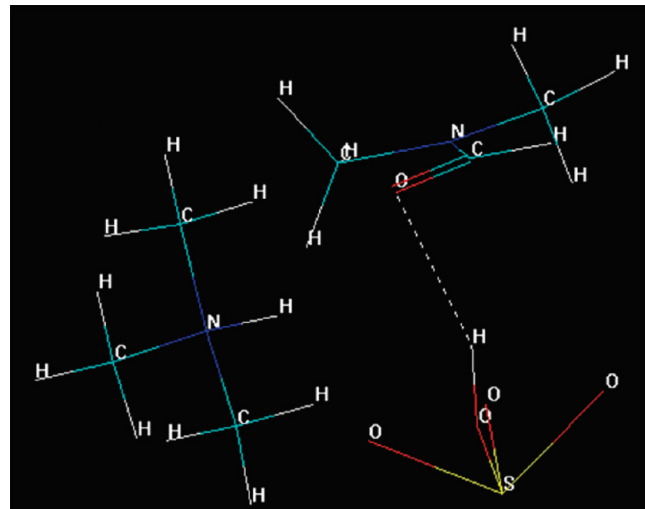


Figure 10. Schematic depiction of the hydrogen bonding interaction between TMAS and DMF molecules, which is predicted by a semi-empirical calculation with the help of Hyperchem 7.

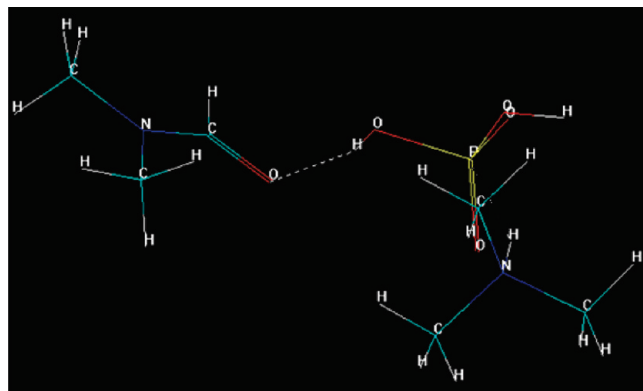


Figure 9. Schematic depiction of the hydrogen bonding interaction between TMAP and DMF molecules, which is predicted by a semi-empirical calculation with the help of Hyperchem 7.

TMAA + DMF at lower temperatures (25 and 30 °C) at the IL-rich concentration region. A minimum value of $\Delta\kappa_s$ is observed at

the IL mole fraction $x_1 = 0.3000$, ≈ 0.3700 , and ≈ 0.3800 for the mixtures of TMAA + DMF, TMAP + DMF, and TMAS + DMF, respectively. As the concentration of the ILs increase and large portion of the DMF molecules are solvated, the amount of bulk solvent decreases which causes a decrease in the compressibility. The negative $\Delta\kappa_s$ of ILs in DMF are also attributed to the strong attractive interactions due to the solvation of the ions in these solvents. The negative values of the $\Delta\kappa_s$ of an ammonium ILs with DMF imply that solvent molecules around the solute are less compressible than the solvent molecules in the bulk solutions. As the mole fraction of IL increases the negative deviation increases sharply up to $x_1 \approx 0.3300$, while with further addition of the ILs there is a decrease in the compressibility graph at all temperature ranges. This might be due to a decrease in attraction of DMF and IL molecules in the IL-rich concentration region, since the interaction between the IL to IL increases and that between IL to DMF decreases (Scheme 2).

On the other hand, the negative $\Delta\kappa_s$ values of DMF-rich region of TMAA + DMF becomes positive $\Delta\kappa_s$ values at higher IL concentration region. These discrepancies vary from IL to IL

(depending on the anion size) and solvent to solvent and also depend on the nature as well as the structural arrangement of IL and solvent. The results in Figure 6 show that the negative $\Delta\kappa_s$ values increase with increasing temperature. Figure 7b depicts that at the lower temperature 25 °C the $\Delta\kappa_s$ values for the TMAA with DMF exhibit an inversion in the sign from negative to positive deviation, indicating that the interaction between TMAA and DMF decreases as the concentration of IL increases at this temperature. The negative $\Delta\kappa_s$ values for TMAS + DMF at 25 °C are higher than those for TMAA or TMAP with DMF mixtures (Figure 7b). The observed strong attractive interactions between IL + DMF are in quite good agreement with the theoretical calculation of hydrogen-bonding interaction of IL + DMF molecules (Figures 8–10).

CONCLUSION

To gain some insight into the new generation of green solvents, we synthesized the novel trimethylammonium ILs, namely, TMAA, TMAP, and TMAS, and studied the influence of the IL, particularly an anion, on the polar solvent. In this paper, densities and ultrasonic sound velocities for three new ILs with DMF have been reported at 25–50 °C under atmospheric pressure. The performed work intends to map the temperature effect on the molecular interaction behavior of an ammonium IL with the DMF molecule. From these measurements, we predicted V^E and $\Delta\kappa_s$ at each temperature as a function of IL concentration. The V^E values for ILs + DMF are negative at all ranges of composition, except TMAP or TMAS with DMF at 25 °C. The negative excess molar volumes reveal that a more efficient packing or attractive interaction occurred when the IL and DMF were mixed. The decrease in the magnitude of the negative V^E values with an increase in IL composition can be attributed to the decrease of hydrogen bonding. The variation in the excess properties depends upon the hydrogen bonding between ILs and DMF. These observed interactions are supported by our theoretical calculations, which are obtained by Hyperchem 7.

The $\Delta\kappa_s$ values for all of the systems are negative over the whole composition range at all studied temperatures, except TMAA + DMF systems. The negative $\Delta\kappa_s$ values of ILs in DMF are also attributed to the strong attractive interactions due to the solvation of the ions in these solvents. The values of V^E and $\Delta\kappa_s$ were correlated by Redlich–Kister equations. The values of V^E and $\Delta\kappa_s$ values increase with increasing temperature. For the first time we show the utility of trimethylammonium ILs and motivate other researchers to explore the different aspects and applications of these novel ILs. These ILs have some additional character compared to the conventional organic solvents in that they are reusable at least five times without loss in their purity.

ASSOCIATED CONTENT

Supporting Information. Mole fraction, density, ultrasonic velocity, isentropic compressibility, and deviation in isentropic compressibility values for the systems of ILs with DMF at various temperatures and atmospheric pressure. This material is available free of charge via the Internet at <http://pubs.acs.org>.

AUTHOR INFORMATION

Corresponding Author

*E-mail: venkatesup@hotmail.com; pvenkatesu@chemistry.du.ac.in. Tel.: +91-11-27666646-142. Fax: +91-11-2766 6605.

ACKNOWLEDGMENT

We are gratefully acknowledged the Council of Scientific Industrial Research (CSIR), New Delhi, through Grant No. 01(2343)/09/EMR-II, Department of Science and Technology (DST), New Delhi, India (Grant No. SR/SI/PC-54/2008) and University Grants Commission (UGC), New Delhi for financial support.

REFERENCES

- (1) Baj, S.; Chrobok, A.; Derfla, S. *Green Chem.* **2006**, *8*, 292–295.
- (2) Seddon, K. R. *J. Chem. Technol. Biotechnol.* **1997**, *68*, 351–356.
- (3) Wasserscheid, P.; Keim, W. *Angew. Chem., Int. Ed.* **2000**, *39*, 3772–3789.
- (4) Van, R. F.; Sheldon, R. A. *Chem. Rev.* **2007**, *107*, 2757–2785.
- (5) Cooper, E. R.; Andrews, C. D.; Wheatley, P. S.; Webb, P. B.; Wormald, P.; Morris, R. E. *Nature* **2004**, *430*, 1012–1016.
- (6) Yoshizawa, M.; Narita, A.; Ohno, H. *Aust. J. Chem.* **2004**, *57*, 139–144.
- (7) Branco, L. C.; Crespo, J. G.; Afonso, C. A. M. *Angew. Chem., Int. Ed.* **2002**, *41*, 2771–2773.
- (8) Dietz, M. L. *Sep. Sci. Technol.* **2006**, *41*, 2047–2063.
- (9) Attri, P.; Venkatesu, P.; Kumar, A. *Phys. Chem. Chem. Phys.* **2011**, *13*, 2788–2796.
- (10) Attri, P.; Venkatesu, P. *Phys. Chem. Chem. Phys.* **2011**, *13*, 6566–6575.
- (11) Seddon, K. R. *Nat. Mater.* **2003**, *2*, 363–365.
- (12) Plechkova, N. V.; Seddon, K. R. *Chem. Soc. Rev.* **2008**, *37*, 123–150.
- (13) Earle, M. J.; Esperanca, J.; Gilea, M. A.; Lopes, J. N. C.; Rebelo, L. P. N.; Magee, J. W.; Seddon, K. R.; Widgren, J. A. *Nature* **2006**, *439*, 831–834.
- (14) Welton, T. *Chem. Rev.* **1999**, *99*, 2071–2083.
- (15) Attri, P.; Reddy, P. M.; Venkatesu, P. *Indian J. Chem. A* **2010**, *49A*, 736–742.
- (16) Attri, P.; Reddy, P. M.; Venkatesu, P.; Kumar, A.; Hofman, T. *J. Phys. Chem. B* **2010**, *114*, 6126–6133.
- (17) Attri, P.; Venkatesu, P.; Kumar, A. *J. Phys. Chem. B* **2010**, *114*, 13415–13425.
- (18) Scammells, P. J.; Scott, J. L.; Singer, R. D. *Aust. J. Chem.* **2005**, *58*, 155–169.
- (19) Seddon, K. R.; Stark, A.; Torres, M. *Pure Appl. Chem.* **2000**, *72*, 2275–2287.
- (20) Blesic, M.; Lopes, J. N. C.; Gomes, M. F. C.; Rebelo, L. P. N. *Phys. Chem. Chem. Phys.* **2010**, *12*, 9685–9692.
- (21) D'Anna, F.; Marullo, S.; Noto, R. *J. Org. Chem.* **2010**, *75*, 767–771.
- (22) Govinda, V.; Attri, P.; Venkatesu, P.; Venkateswarlu, P. *Fluid Phase Equilib.* **2011**, *304*, 35–43.
- (23) Mokhtaran, B.; Sharifi, A.; Mortaheb, H. R.; Mirzaei, M.; Mafi, M.; Sadeghian, F. *J. Chem. Thermodyn.* **2009**, *41*, 323–329.
- (24) Wagner, M.; Stanga, O.; Schröer, W. *Phys. Chem. Chem. Phys.* **2003**, *5*, 3943–3950.
- (25) Ortega, J.; Vreekamp, R.; Marrero, E.; Penco, E. *J. Chem. Eng. Data* **2007**, *52*, 2269–2276.
- (26) Fröba, A. P.; Kremer, H.; Leipertz, A. *J. Phys. Chem. B* **2010**, *112*, 12420–12430.
- (27) Wang, J.; Tian, Y.; Zhuo, K. *Green Chem.* **2003**, *5*, 618–622.
- (28) Geppert-Rybczyńska, M.; Heintz, A.; Lehmann, J. K.; Gorus, A. *J. Chem. Eng. Data* **2010**, *55*, 4114–4120.
- (29) Wang, J.; Wang, H.; Zhang, S.; Zhang, H.; Zhao, Y. *J. Phys. Chem. B* **2007**, *111*, 6181–6188.
- (30) Firestone, A.; Dzielawa, J. A.; Zapol, P.; Curtiss, L. A.; Seifert, S.; Dietz, M. L. *Langmuir* **2002**, *18*, 7258–7260.
- (31) Law, G.; Watson, P. R. *Langmuir* **2001**, *17*, 6138–6141.
- (32) Zhang, Z.; Wu, W.; Gao, H.; Han, B.; Wang, B.; Huang, Y. *Phys. Chem. Chem. Phys.* **2004**, *6*, 5051–5055.

- (33) Iglesias-Otero, M. A.; Troncoso, J.; Carballo, E.; Romaní, L. *J. Chem. Eng. Data* **2008**, *53*, 1298–1301.
- (34) Wang, J.; Tian, Y.; Zhao, Y.; Zhuo, K. *Green Chem.* **2003**, *5*, 618–622.
- (35) Venkatesu, P. *Rev. Fluid Phase Equilib.* **2010**, *289*, 173–191.
- (36) Žagar, E.; Žigon, M. *Polymer* **2000**, *41*, 3513–3521.
- (37) Kang, Y. K.; Park, H. S. *J. Mol. Struct. (THEOCHEM)* **2004**, *676*, 171–176.
- (38) García, B.; Alcalde, R.; Leal, J. M.; Matos, J. S. *J. Chem. Soc., Faraday Trans.* **1997**, *93*, 1115–1118.
- (39) Venkatesu, P.; Lee, M. J.; Lin, H. M. *J. Chem. Thermodyn.* **2005**, *53*, 996–1002.
- (40) Venkatesu, P.; Rao, M. V. P. *J. Chem. Eng. Data* **1997**, *42*, 90–92.
- (41) Venkatesu, P.; Rao, M. V. P. *J. Chem. Thermodyn.* **1998**, *30*, 207–213.
- (42) Riddick, J. A.; Bunger, W. B.; Sakano, T. K. *Organic solvents*, 4th ed.; Wiley-Interscience: New York, 1986.
- (43) Venkatesu, P.; Rao, M. V. P.; Prasad, D. H. L.; Ravikumar, Y. V. L. *Thermochim. Acta* **1999**, *342*, 73–78.
- (44) Venkasteu, P.; Sekhar, C. G.; Rao, M. V. P.; Hofman, T. *Thermochim. Acta* **2006**, *443*, 62–71.
- (45) Attri, P.; Pal, M. *Green Chem. Lett. Rev.* **2010**, *3*, 249–256.
- (46) Weng, J.; Wang, C.; Li, H.; Wang, Y. *Green Chem.* **2006**, *8*, 96–99.
- (47) Huq, F.; Yu, J. Q. *J. Mol. Model.* **2002**, *8*, 81–86.
- (48) Jorgensen, W. L.; Chandrasekhas, J.; Madura, J. D.; Impey, R. W.; Klein, M. L. *J. Chem. Phys.* **1983**, *79*, 926–935.
- (49) Schmid, E. D.; Odbek, E. *Can. J. Chem.* **1985**, *63*, 1365–1371.
- (50) Bonhote, P.; Dias, A. P.; Papageorgiou, N.; Kalyanasundaram, K.; Gratzel, M. *Inorg. Chem.* **1996**, *35*, 1168–1178.
- (51) Pinkert, A.; Ang, K. L.; Marsh, K. N.; Pang, S. *Phys. Chem. Chem. Phys.* **2011**, *13*, 5136–5143.
- (52) Fredlake, C. P.; Crosthwaite, J. M.; Hert, D. G.; Aki, S. N. V. K.; Brennecke, J. F. *J. Chem. Eng. Data* **2004**, *49*, 954–964.
- (53) Wilkes, J. S. *J. Mol. Catal., A: Chem.* **2004**, *214*, 11–17.
- (54) Marsh, K. N.; Boxall, J. A.; Lichtenthaler, R. *Fluid Phase Equilib.* **2004**, *219*, 93–98.